Archives of Toxicology (2019) 93:2617–2634
https://doi.org/10.1007/s00204-019-02539-x

IN VITRO SYSTEMS

The new psychoactive substance 3-methylmethcathinone (3-MMC or metaphedrone) induces oxidative stress, apoptosis, and autophagy in primary rat hepatocytes at human-relevant concentrations

Diana Dias da Silva[1] · Bárbara Ferreira[1] · Rita Roque Bravo[1] · Rita Rebelo[1] · Tomás Duarte de Almeida[1] · Maria João Valente[2] · João Pedro Silva[1] · Félix Carvalho[1] · Maria de Lourdes Bastos[1] · Helena Carmo[1]

Received: 18 March 2019 / Accepted: 14 August 2019 / Published online: 29 August 2019

Abstract

3-Methylmethcathinone (3-MMC or metaphedrone) has become one of the most popular recreational drugs worldwide after the ban of mephedrone, and was recently deemed responsible for several intoxications and deaths. This study aimed at assessing the hepatotoxicity of 3-MMC. For this purpose, Wistar rat hepatocytes were isolated by collagenase perfusion, cultured and exposed for 24 h at a concentration range varying from 31 nM to 10 mM 3-MMC. The modulatory effects of cytochrome P450 (CYP) inhibitors on 3-MMC hepatotoxicity were evaluated. 3-MMC-induced toxicity was perceived at the lysosome at lower concentrations (NOEC 312.5 µM), compared to mitochondria (NOEC 379.5 µM) and cytoplasmic membrane (NOEC 1.04 mM). Inhibition of CYP2D6 and CYP2E1 diminished 3-MMC cytotoxicity, yet for CYP2E1 inhibition this effect was only observed for concentrations up to 1.3 mM. A significant concentration-dependent increase of intracellular reactive species was observed from 10 µM 3-MMC on; a concentration-dependent decrease in antioxidant glutathione defences was also observed. At 10 µM, caspase-3, caspase-8, and caspase-9 activities were significantly elevated, corroborating the activation of both intrinsic and extrinsic apoptosis pathways. Nuclear morphology and formation of cytoplasmic acidic vacuoles suggest prevalence of necrosis and autophagy at concentrations higher than 10 µM. No significant alterations were observed in the mitochondrial membrane potential, but intracellular ATP significantly decreased at 100 µM. Our data point to a role of metabolism in the hepatotoxicity of 3-MMC, which seems to be triggered both by autophagic and apoptotic/necrotic mechanisms. This work is the first approach to better understand 3-MMC toxicology.

Keywords 3-Methylmethcathinone (3-MMC or metaphedrone) · Synthetic cathinone · Hepatotoxicity · Oxidative stress · Apoptosis · Autophagy

Introduction

In the context of the new psychoactive substances (NPS), mephedrone (4-methylmethcathinone, 4-MMC) became widely used as a surrogate compound for 3,4-methylenedioxymethamphetamine (MDMA), being the first example of a NPS that resulted in a widespread use (Green et al. 2014). Similar to the classic amphetamines, this synthetic cathinone belongs to the phenethylamine family. As the production and trafficking of mephedrone was forbidden in most European countries (ACMD 2010; EMCDDA 2011), the search for other drugs with comparable stimulant effects proceeded, and other mephedrone-like substitutes quickly showed up on the grey NPS market; a relevant example of such cases is 3-methylmethcathinone (3-MMC) that was first encountered in 2012, in Sweden (Backberg et al. 2015), but rapidly

✉ Diana Dias da Silva
diana.dds@gmail.com

✉ Helena Carmo
helenacarmo@ff.up.pt

[1] UCIBIO, REQUIMTE, Laboratory of Toxicology, Department of Biological Sciences, Faculty of Pharmacy, University of Porto, Rua Jorge Viterbo Ferreira, 228, 4050-313 Porto, Portugal

[2] UCIBIO, REQUIMTE, Laboratory of Biochemistry Department of Biological Sciences, Faculty of Pharmacy, University of Porto, Rua Jorge Viterbo Ferreira, 228, 4050-313 Porto, Portugal

spread all over Europe (Ferreira et al. 2019). As a structural isomer of mephedrone, this synthetic cathinone has also similar psychostimulant properties to amphetamines, inducing euphoria, increased physical energy, alertness, feelings of empathy and enhanced awareness, among other symptoms (Adamowicz et al. 2016; Sande 2016). Users described comedown effects of 3-MMC as softer than those of mephedrone and, therefore, preferable (Adamowicz et al. 2016). Self-reported dosages range from 50 to 150 mg and many users report binge administrations to prolong the euphoric experience, accounting up to doses as high as 2 g consumed during a single session or within a few hours (Ameline et al. 2018; Sande 2016). Users claim the onset of the first effects between 20 and 30 min after oral administration and the peak effects are experienced after 50 min, lasting up to 3–4 h (Ameline et al. 2018; Bluelight 2012; Erowid 2013).

There are currently no systematic studies elucidating the potential toxicological effects of 3-MMC, and the information available pertains clinical data from emergency episodes (Romanek et al. 2017), data retrieved from websites where users self-report drug experiences (Bluelight 2012; Erowid 2013) and forensic reports of fatal and non-fatal drug-related cases (Adamowicz et al. 2014, 2016; Jamey et al. 2016). Tachycardia, hallucinations, agitation, reduced level of consciousness, hyperthermia, and seizures, are among the main reported adverse effects (Ferreira et al. 2019). These data suggest that 3-MMC is as dangerous as mephedrone, but knowledge on the inherent toxicological mechanisms are solely speculated based on those for similar drugs of abuse.

The liver is one of the main sites of cathinones' metabolism (Valente et al. 2014), and therefore a relevant target for their deleterious effects, particularly when administered per os. Accordingly, a relevant number of cases evidencing liver injury or abnormal liver function as clinical adverse effects associated with mephedrone abuse have been reported (James et al. 2011; Kasick et al. 2012; Schifano et al. 2012). In addition, mephedrone was shown to induce liver damage in animal models (Joanna et al. 2017; Tarkowski et al. 2018), and both in vitro and in vivo studies demonstrate that hepatic cells are able to metabolise this cathinone derivative, originating metabolites (including hydroxylated metabolites) that have the potential to be more toxic than the parent compound (Martinez-Clemente et al. 2013; Pedersen et al. 2013b). Further relevance on the hepatotoxic effects of the drug stems from the fact that drug abusers regularly co-ingest other illicit drugs and alcohol, which could potentiate liver toxicity, particularly in a long-term perspective. Thus, the aims of this study were to assess the mechanistic pathways of toxicity of the structural isomer of mephedrone 3-MMC in hepatocytes, and to correlate putative detrimental effects with CYP450 activity. Due to the important role of liver in metabolism, it is possible that the drug may also undergo bioactivation with production of metabolites with higher toxicity, compromising the functionality of the organ and of the overall health of the abuser.

Materials and methods

Chemicals

The hydrochloride salt of 3-MMC was purchased online (website currently unavailable). Chemical purity and identity of the drug were verified by mass spectrometry, NMR and elemental analysis. Analytical data were consistent with the assigned structure, with about 98% purity.

Unless stated otherwise, all other chemicals were purchased from Sigma-Aldrich (Lisbon, Portugal) and all the cell culture reagents from Gibco® (Alfagene, Lisbon, Portugal).

Animals

Male Wistar Han rats with a body weight of 150–250 g were kept in sterile facilities under controlled temperature (20 ± 2 °C), humidity (40–60%), and light (12-h light/dark cycle) conditions, and were fed with sterile standard rat chow and tap water ad libitum. Isolation of hepatocytes was always conducted between 8:00 and 10:00 a.m. Surgical procedures were performed after rat anaesthesia and analgesia induced by an i.p. injection of a combination of 100 mg/kg ketamine (Clorketam® 1000, Vétoquinol, France) and 20 mg/kg xylazine (Rompun® 2%, Bayer HealthCare, Germany), and maintained through inhalation of isoflurane vapour (IsoVet® 1000 mg/g, B. Braun VetCare, Germany). This study was performed at the highest standards of ethics after approval by the local Ethical Committee for the Welfare of Experimental Animals (University of Porto-ORBEA) and by the national authority Direção-Geral de Alimentação e Veterinária (DGAV). Housing and all experimental procedures were performed by investigators accredited for laboratory animal use in accordance with the Portuguese and European legislation (law DL 113/2013, Guide for Animal Care; Directives 86/609/EEC and 2010/63/UE) under strict supervision of veterinary physicians.

Isolation of primary rat hepatocytes

Isolation of hepatocytes was performed using a modified two-step perfusion of the liver, as previously described by Dias da Silva et al. (2017) with some modifications. The liver was perfused in situ via the portal vein, with a sterile EGTA-buffer at 37 °C, for approximately 10–15 min. The chelator promoted the irreversible cleavage of the hepatic desmosomes (junctional complexes) through calcium sequestration. The EGTA-buffer consisted of 248 mL

glucose solution (9 g/L D-glucose), 40 mL Krebs–Henseleit buffer (60 g/L NaCl, 1.75 g/L KCl, and 1.6 g/L KH_2PO_4; adjusted to pH 7.4), 40 mL HEPES buffer I (60 g/L HEPES; adjusted to pH 8.5), 30 mL MEM non-essential amino acid solution (100×), 30 mL MEM Amino Acids (10×) solution, 4 mL glutamine solution (7 g/L L-glutamine), and 1.6 mL EGTA solution (47.5 g/L EGTA; dissolved by addition of NaOH, adjusted to pH 7.6). Subsequently, hepatic collagen was hydrolysed by liver perfusion for 10–15 min with a sterile collagenase buffer supplemented with calcium (collagenase cofactor), at 37 °C. The collagenase buffer consisted of 155 mL glucose solution, 25 mL Krebs–Henseleit buffer, 25 mL HEPES buffer I, 15 mL MEM non-essential amino acid solution (100×), 15 mL MEM amino acids (10×) solution, 10 mL $CaCl_2$ solution (19 g/L $CaCl_2.2H_2O$), 2.5 mL glutamine solution, and ~ 300 U/mL collagenase type IA from *Clostridium histolyticum* (dissolved immediately before use). After perfusion, the liver was dissected, removed from the animal, and the hepatic capsule gently disrupted in a sterile suspension buffer [124 mL glucose solution, 20 mL KH buffer, 20 mL HEPES buffer II (60 g/L HEPES; adjusted to pH 7.6), 15 mL MEM non-essential amino acid solution (100×), 15 mL MEM amino acids (10×) solution, 2 mL glutamine solution, 1.6 mL $CaCl_2$ solution, 0.8 mL $MgSO_4$ solution (24.6 g/L $MgSO_4{\cdot}7H_2O$), and 400 mg bovine serum albumin (BSA)]. The obtained suspension was purified by three low-speed centrifugations at 50 *g*, for 2 min, at 4 °C. The viability of isolated hepatocytes was always above 85%, as assessed by the trypan blue exclusion method.

Culture of primary rat hepatocytes

A suspension of 5×10^5 viable cells/mL in culture medium was seeded onto the central 60 wells of 96-well plates (5×10^4 cells/well) or onto 6-well plates ($1x10^6$ cells/well) pre-coated with collagen G (Biochrom Ltd.). Cell culture medium consisted of William's E medium (Sigma-Aldrich, Lisbon, Portugal) supplemented with 10% heat-inactivated foetal bovine serum (FBS), 5 µg/mL insulin solution from bovine pancreas (Sigma-Aldrich, Lisbon, Portugal), 50 nM dexamethasone (Sigma-Aldrich, Lisbon, Portugal), 1% antibiotic solution (10,000 U/mL penicillin; 10,000 µg/mL streptomycin), 100 µg/mL gentamicin, and 250 ng/mL amphotericin B. After seeding, primary rat hepatocytes were left to adhere overnight at 37 °C, in an atmosphere of 5% CO_2. On the next day, cells were exposed to the test drug.

Drug challenge

Stock solutions of 3-MMC were extemporaneously prepared in Hank's balanced salt solution (HBSS) and further diluted in cell culture medium. For the cell viability experiments, the primary rat hepatocyte cultures were exposed to at least 22 concentrations ranging from 31 nM to 10 mM, enabling to obtain complete concentration vs. effect curves (i.e. from 0 to 100% of effect). All the other assays performed to elucidate the mechanisms responsible for the elicited hepatotoxicity were conducted at four test 3-MMC concentrations: 1 µM, 10 µM, 100 µM and 500 µM. These concentrations were chosen to allow the investigation of the toxicological mechanisms triggered by the drug at different cytotoxic effect levels. None of these test concentrations was able to induce significant mortality as assessed by the MTT assay ($p > 0.05$), precluding interference with results on the endpoints evaluated. In addition, the lowest tested concentrations (≤ 10 µM) are in line with the blood concentration found in human fatal intoxications (Adamowicz et al. 2016), as further discussed. All drug exposures were performed for 24 h, at 37 °C, in a humidified, 5% CO_2 atmosphere. Solvent and negative controls were always assessed parallel to drug incubations. Comparison between solvent (HBSS at a maximum of 5%, as tested) and negative controls (cells treated with only cell culture medium) showed no statistically significant differences ($p > 0.05$).

Cell viability by the 3-(4,5-dimethylthiazol-2-yl)-2,5-diphenyltetrazolium bromide (MTT) reduction assay

The cytotoxicity of the drug was evaluated in hepatocytes seeded onto 96-well plates using the 3-(4,5-dimethylthiazol-2-yl)-2,5-diphenyltetrazolium bromide (MTT) reduction assay, as described before (Dias-da-Silva et al. 2015). The assay assesses cell metabolic viability indirectly through the measurement of the activity of reductases that convert yellow soluble MTT into purple insoluble formazan salts. As MTT can only be reduced when these enzymes are active, the reaction is used as an indicator of the cell metabolic competence and, therefore, viability. Each concentration was tested in triplicate in four independent experiments. Data were normalised to positive (1% Triton X-100) and negative controls and results were graphically presented as percentage of cell death vs. concentration (mM).

Cytochrome P450 inhibition

In order to determine the influence of CYP metabolism in the toxicity of the drug, different CYP isoforms of primary rat hepatocytes were inhibited previous to and during exposure to the test drug. Briefly, cells were incubated for 1 h with four CYP inhibitors: metyrapone (CYP2E1 inhibitor) at 500 µM, quinidine (CYP2D6 inhibitor) at 10 µM, ketoconazole (CYP3A4 inhibitor) at 1 µM, and 1-aminobenzotriazole (ABT; general CYP inhibitor) at 1 mM. Each inhibitor concentration was selected in order to induce inhibition without eliciting cytotoxicity, as already optimised for our

experimental settings (cellular model and viability assay) (Dias-da-Silva et al. 2015). Then, cells were co-incubated with these inhibitors and the test drug, during 24 h, at 37 °C. Afterwards, cell viability was evaluated using the MTT assay as described, and data from four independent experiments (each condition tested in six replicates) were normalised to positive (1% Triton X-100) and negative controls. Inhibitor controls (only inhibitor in cell culture medium) were performed and compared to negative controls to ensure that no cytotoxicity derived from these treatments.

Quantification of 3-MMC by gas chromatography–mass spectrometry (GC–MS)

The culture medium from hepatocyte exposures to 3-MMC was collected and 500 µL were submitted to a QuEChERS extraction. Briefly, following addition of 50 µL of 500 ng/mL phenylpropanolamine (internal standard, IS), samples' pH was adjusted to > 11, and 3 mL of tert-butylmethylether, 750 mg of $MgSO_4$ anhydrous and 100 mg of NaCl were subsequently added. After vortex homogenisation for 30 s and centrifugation at 500*g* for 3 min, the supernatant was transferred into a new vial and evaporated to dryness under N_2 stream. Then, derivatisation with heptafluorobutyric acid anhydride (HFBA) was performed using a procedure adapted from Jamey et al. (2016). Accordingly, 50 µL of ethyl acetate and 50 µL of HFBA were added to the dry residue, vortex mixed for 30 s and heated at 60 °C for 30 min. After cooling to room temperature, the sample was evaporated to dryness under N_2 stream and the residue dissolved in 100 µL of ethyl acetate. GC–MS analysis was carried out using a HP 6890 series gas chromatograph (Agilent, Little Falls, DE, USA) coupled to an Agilent 5973 Network MSD (mass-selective detector). A capillary column Rxi-5sil (30 m × 0.25 mm × 0.25 µm) from RESTEK was employed for the separation. The software used in the control, acquisition and data treatment was Agilent MSD Productivity ChemStation for GC and GC/SD Chemstation from Agilent Technologies (Santa Clara, CA, USA). Helium C-60 (Gasin, Portugal), at a constant flow rate of 1 mL/min, was used as the carrier gas. The injection of 1 µL of derivatised extracts was manually done in the splitless mode at 270 °C. The column oven temperature was maintained at 80 °C for 1 min, and then raised to 290 °C at 25 °C/min, and held at 290 °C for 5.6 min, with a total run of 15 min. This method was adapted from Adamowicz (2017) and Adamowicz et al. (2014). The transfer line temperature was 280 °C, and the electron energy was 70 eV. During the first 4 min, the ionisation was maintained off to avoid solvent overloading. Data were collected at *m/z* 40–500. Mass spectra acquisition was performed between 4 and 15 min after the injection of the sample. Full scan mode allowed the detection of all ions and was used for the characterisation of the spectra and identification of compounds; selected ion monitoring (SIM) mode allowed quantification of compounds. The ions selected for monitoring were chosen based on the specificity and abundance on the mass spectrum. The identification of each analyte in the samples was made by comparing the retention times and the mass spectra (relative abundance of the ions) of the standards with those of the peaks obtained when injecting the samples under the same chromatographic conditions. For identification, the ions chosen were as follows: IS *m/z* = 330 and 275; 3-MMC *m/z* = 373, 254 and 210; while for quantification IS *m/z* = 240 and 3-MMC *m/z* = 119 were used. Retention time was 6.70 min for 3-MMC and 5.55 min for IS.

Linearity, precision, accuracy and recovery were all within the accepted values for these parameters. Stock solutions of 3-MMC and IS were prepared at 1 mg/mL in methanol and stored at − 20 °C. All intermediate dilutions and working solutions were also prepared in methanol. The limit of detection (LOD) and limit of quantitation (LOQ) were determined based on the signal-to-noise ratio, by progressively diluting (factor of 2) a 125 ng/mL working calibrator; a signal-to-noise ratio of 3 and 10, respectively, were considered acceptable for estimating LOD at 3.5 ng/mL and LOQ at 7 ng/mL. Working calibrators at 125, 175, 250, 500 and 1000 ng/mL in cell culture medium were prepared and stored at − 20 °C. Regression curves were obtained by plotting the peak-area ratio between the analyte and the IS against analyte concentrations. Linearity of the calibration curves was evaluated by the coefficient of determination (R^2) and considered good ($R^2 = 0.9980$) in the concentration range tested (12.5–100 ng/mL). The extraction efficiency was calculated comparing the peak-area ratios of analyte to IS for extracted and non-extracted samples at 12.5 ng/mL (85%), 25 ng/mL (94%) and 50 ng/mL (96%) of 3-MMC, and showed recovery values that were at the acceptable criteria of 100 ± 20% for this parameter. Data from four independent experiments (each condition tested in six replicates) were presented as percentage of metabolised 3-MMC.

Cell viability by the lactate dehydrogenase (LDH) leakage assay

Cytoplasmic membrane integrity, evaluated through the lactate dehydrogenase (LDH) leakage assay, also offers a feasible indication of cell viability. As LDH is a cytoplasmic oxidoreductase, its presence in the extracellular medium is indicative of alterations in membrane permeability and consequently in cell integrity. The enzyme catalyses the reversible conversion of pyruvate to lactate, in the presence of nicotinamide adenine dinucleotide (NADH), which is in turn oxidised into NAD^+. At the end of the incubation period, 10 µL of cell culture medium was transferred into a 96-well plate and added with 200 µL of freshly prepared 0.15 mg/

mL β-NADH solution. Immediately before the absorbance reading, 25 µL of 2.5 mg/mL sodium pyruvate solution were added to start the reaction. Both β-NADH and sodium pyruvate solutions were prepared in potassium phosphate buffer (50 mM KH_2PO_4, pH 7.4). The kinetics of the oxidation of β-NADH to NAD^+ was followed by reading the absorbance at 340 nm, every 16 s, for 3 min, using an automatic plate reader Power Wave X™ (BioTek Instruments, Inc.). The data obtained in six replicates from four independent experiments were normalised to the negative controls and results were graphically presented as percentage of positive controls (1% Triton X-100).

Cell viability by the neutral red (NR) inclusion assay

To provide supplementary cell viability data, we performed the neutral red (NR) uptake assay as described by Arbo et al. (2014) with minor modifications. This assay is based on the ability of viable cells to incorporate and bind the weak cationic dye NR, which penetrates the cells by non-ionic diffusion, accumulating in lysosomes by interaction with anionic sites in the organelle matrix. At the end of the incubation period, the exposure medium of the hepatocytes seeded onto 96-well plates was replaced by 50 µg/mL NR solution, prepared in HBSS. The cells were incubated at 37 °C in a humidified, 5% CO_2 atmosphere for 30 min, allowing the lysosomes of viable cells to take up the dye. Cells were then carefully washed twice with 200 µL of HBSS to eliminate extracellular dye, and lysed with 100 µL of lysis solution (50% ethanol:1% glacial acetic acid:49% water). The absorbance was measured at 540 nm in a multi-well plate reader BioTek Synergy™ HT (BioTek Instruments, Inc.). Data, obtained in triplicates from four independent experiments, were normalised to positive (1% Triton X-100) controls and results were graphically presented as percentage of negative controls.

Intracellular reactive oxygen (ROS) and nitrogen (RNS) species

The assessment of intracellular ROS and RNS was performed using the 2′,7′-dichlorodihydrofluorescein diacetate (DCFH-DA) fluorescence assay, as described by Dias da Silva (2014a). Briefly, hepatocytes seeded onto 96-well plates were exposed for 30 min to 10 µM DCFH-DA, at 37 °C, protected from light. Afterwards, the cells were washed with HBSS and incubated with the test drug, at 37 °C for 24 h. The fluorescence was recorded at the end of the incubation period using a fluorescence microplate reader BioTek Synergy™ HT (BioTek Instruments, Inc.), set at 485 nm excitation and 530 nm emission. Data acquired from four independent experiments (each condition tested in six replicates) were normalised to control conditions (only cell culture medium).

Total (tGSH), reduced (GSH), and oxidised (GSSG) glutathione

Primary rat hepatocytes exposed to the drug on 6-well plates were washed with HBSS with calcium and magnesium at the end of the incubation period, and then precipitated with 10% perchloric acid for 20 min, at 4 °C. Cells were scrapped and the obtained suspension was centrifuged at 13,000*g* for 5 min, at 4 °C. The supernatant was collected and stored at − 80 °C until further determinations. The cell pellet was resuspended in 1 M NaOH and used to quantify protein, as described below. After thawing, the supernatants were neutralised with an equal volume of 0.76 M $KHCO_3$ and centrifuged at 13,000*g* for 10 min, at 4 °C. Then, supernatants were used to determine total glutathione (tGSH), oxidised glutathione (GSSG) and ATP.

As previously described (Martins et al. 2018), tGSH was measured through the 5,5-dithio-bis(2-nitrobenzoic acid) (DTNB)-GSSG reductase-recycling assay. Briefly, 100 µL of each sample supernatant, blank and standards were transferred into a 96-well plate, followed by the addition of 65 µL reagent solution (72 mM phosphate buffer, 0.69 mM NADPH, and 4 mM DTNB). The plates were incubated for 15 min, at 30 °C, in a multi-well plate reader (Power Wave X™, BioTek Instruments, Inc.) and then 40 µL of a 10 U/mL glutathione reductase solution were added. The absorbance was read at 415 nm every 10 s, for 3 min, in kinetic mode, allowing to follow the formation of 5-thio-2-nitrobenzoic acid (TNB). The sample results were compared with a standard curve, performed in every independent experiment. As 2-vinylpyridine blocks GSH, the same protocol was used for the quantification of GSSG, following sample incubation with 10 µL 2-vinylpyridine for 1 h, at 4 °C. Data from four independent experiments (each condition tested in two replicates) were normalised to the protein content of each sample, and the concentration of intracellular redGSH was calculated using the formula $\text{redGSH} = \text{tGSH} - 2 \times \text{GSSG}$.

Intracellular adenosine triphosphate (ATP)

A bioluminescence method was used for measuring intracellular ATP, as previously described (Martins et al. 2018). Samples were prepared as described above for the determination of glutathione. Afterwards, 75 µL of each sample supernatant, standard, or blank were transferred into a white 96-well plate. Then, 75 µL of a luciferin–luciferase solution (0.15 mM luciferin; 30,000 light units luciferase/mL; 10 mM $MgSO_4$; 50 mM glycine; 1 mM Tris; 0.55 mM EDTA; 1% BSA) were added and the emitting light intensity was measured using a luminescence plate reader BioTek

Synergy™ HT (BioTek Instruments, Inc.). The results from four independent experiments (each condition tested in two replicates) were compared to a standard curve performed in every experiment and normalised to the protein content.

Determination of protein

The protein content in the samples for normalisation of ATP, tGSH and GSSG contents was measured through the method of Lowry et al. (1951). Accordingly, 50 µL of each sample, standard, or blank were transferred into a 96-well plate, in triplicate, and added of 100 µL reagent A (14.7 mL of 2% Na_2CO_3, 0.15 mL of 2% $KNaC_4H_4O_6{\cdot}4H_2O$, and 0.15 mL of 1% $CuSO_4{\cdot}5H_2O$, extemporaneously prepared). The plate was incubated in the dark for 10 min, at room temperature, followed by the addition of 100 µL of reagent B (Folin and Ciocalteu's phenol reagent, diluted 15× in purified water). The plate was incubated for 10 min, under light protection, at room temperature, and the absorbance was measured at 750 nm in a 96-well microplate reader (Power Wave X™, BioTek Instruments, Inc.). Protein standards (31.25–500 µg BSA/mL) were prepared in 1 M NaOH.

Mitochondrial membrane potential ($\Delta\psi m$)

Mitochondrial integrity was evaluated using tetramethylrhodamine ethyl ester (TMRE), a positive-charged dye that is included solely in active mitochondria. As described by Dias da Silva et al. (2013a), following drug exposure, the medium was aspirated and cells seeded onto 96-well plates were washed with HBSS (no calcium, no magnesium) and incubated with 2 µM TMRE prepared in fresh culture medium, for 30 min, protected from light. After the incubation period, cells were washed twice with HBSS (no calcium and no magnesium) and the fluorescence was quantified using a fluorescence microplate reader BioTek Synergy™ HT (BioTek Instruments, Inc.), set at 544 nm excitation and 590 nm emission. Data from four independent experiments (each condition tested in six replicates) were normalised to negative controls.

Caspase-8, -9, and -3 activities

The activity of pro-apoptotic caspases-3, -8 and -9 was evaluated in hepatocytes seeded onto 6-well plates, following drug exposure, according to the procedure described by Martins et al. (2018). The incubation medium was discarded, the cells washed with HBSS and added of 150 µL lysis buffer (50 mM HEPES, 0.1 mM EDTA, 0.1% CHAPS and 1 mM DTT; pH 7.4). The plates were then incubated at 4 °C for 30 min. Following this period, the cells were scraped, collected into microcentrifuge tubes, and centrifuged at 13,000 rpm for 10 min, at 4 °C. Then, 50 µL of the resulting supernatant were collected into a 96-well plate and added of 200 µL assay buffer (100 mM NaCl, 50 mM HEPES, 0.1 mM EDTA, 10% Glycerol, 0.1% CHAPS and 10 mM DTT). The reaction was started by adding 5 µL of caspase-3 (Ac-DEVD-pNA; 4 mM in DMSO), caspase-8 (Ac-IETD-pNA; 10 mM in DMSO), or caspase-9 (Ac-LEHD-pNA; 10 mM in DMSO) peptide substrate. The plates were then covered with parafilm and aluminium foil and incubated at 37 °C for 24 h. After this time, the absorbance was measured at 405 nm in a multi-well plate reader BioTek Synergy™ HT (BioTek Instruments, Inc.). Data were normalised to the amount of protein of each sample. The protein content in the cytoplasmic fraction was quantified using the DC™ protein assay kit (Bio-Rad Laboratories, CA, USA), as described by the manufacturer. Results from four independent experiments (each condition tested in two replicates) were expressed as percentage of negative controls.

Hoechst 33342/propidium iodide (PI) fluorescent staining

Apoptotic hepatocytes were identified based on chromatin morphology, as previously described by Valente et al. (2016b), using Hoechst 33342, a cell-permeant nuclear counterstain that emits blue fluorescence when bound to DNA, and propidium iodid (PI), a membrane impermeant nuclear dye that emits red fluorescence only in dead cells. Briefly, after washing hepatocytes seeded into 6-well plates with HBSS (without calcium and magnesium), cells were incubated with 50 µM PI for 15 min, under light protection, rinsed twice, incubated with a 5 µg/mL Hoechst 33342 solution for 5 min, and observed under an inverted fluorescent microscope Nikon Eclipse Ti (Nikon, Amsterdam, Netherlands), at an original magnification of 200×. Photographs of randomly chosen fields representative of the results obtained in two independent experiments are presented.

Fluorescence microscopy with acridine orange (AO) staining

Following exposure, hepatocytes were incubated with 5 µg/mL acridine orange (AO) for 20 min, at 37 °C, to detect acidic vesicular organelles (AVOs) formation (Valente et al. 2017a). AO is a lysosomotropic dye that emits green/yellow/orange/red fluorescence in a pH-dependent manner. At neutral pH, AO is a hydrophobic green molecule, while within acidic organelles it becomes protonated and forms aggregates that emit bright yellow to red fluorescence. Following incubation with AO, cells were rinsed three times with HBSS and observed under an inverted fluorescence microscope Nikon Eclipse Ti (Nikon, Amsterdam, Netherlands), at an original magnification of 200×. Photographs of

randomly chosen fields representative of the results obtained in two independent experiments are presented.

Statistical analysis

The normalised MTT, LDH, and NR assays data were fitted to the dosimetric logit model, which was chosen based on a statistical goodness-of-fit principle (Dias da Silva et al. 2013b): $y = \theta_{max}/\{1 + \exp[-\theta_1 - \theta_2 * \log(x)]\}$, where θ_{max} is the maximal observed effect, θ_1 is the parameter for location, θ_2 is the slope parameter and x is the concentration of test drug. To compare concentration–response curves, overlapping of the 95% confidence intervals was used in addition to the extra sum-of-squares F test. The lowest observed effect concentrations (LOECs) and no observed effect concentrations (NOECs) were calculated by testing a trend in concentration effects against control by applying hypothesis-testing procedures (unpaired t tests) (Silva et al. 2007), which allowed the estimation of LOECs. Consequently, the next lower tested concentrations could be assigned as NOEC values. Results from the determination of ROS/RNS, GSH/GSSG, Δψm, caspase-3, -8, -9 activities, and ATP were presented as mean ± standard error of the mean (SEM) from four independent experiments. Normality of the data distribution was confirmed by the Shapiro–Wilk normality tests. Statistical comparisons between groups were performed by one-way analysis of variance (ANOVA) followed by Dunnett's multiple comparison test. Solvent and negative control values were compared by the Student's t test. In all cases, significance was accepted at p values < 0.05. All statistical calculations were performed using GraphPad Prism software, version 7.0 (GraphPad Software, San Diego, CA, USA).

Results

Lysosome was the most sensitive organelle to 3-methylmethcathinone (3-MMC)-induced toxicity, followed by mitochondria and by the cytoplasmic membrane

Cellular viability was evaluated by three different assays (LDH leakage, NR uptake, and MTT reduction assays). The comparison of the obtained results provided information about the relative sensitivity of the target organelles, when the cells were exposed to 3-MMC. As shown in Fig. 1, 3-MMC-induced toxicity was perceived in the lysosome at lower concentrations (NR LOEC 379.5 µM) than those needed to cause damage to mitochondria (MTT LOEC 531.2 µM) and cytoplasmic membrane (LDH LOEC 1.32 mM). Accordingly, the potency of 3-MMC for inducing 50% of cell death was also distinct among the different assays (Table 1; NR EC_{50} 1.36 mM; MTT EC_{50} 1.68 mM; LDH EC_{50} 3.13 mM).

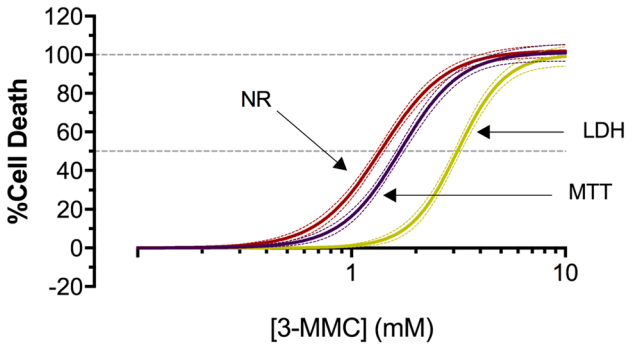

Fig. 1 Cell death of primary rat hepatocytes after 24-h exposure at 37 °C to 3-methylmethcathinone (3-MMC), obtained in the lactate dehydrogenase leakage assay (LDH, data displayed in yellow), neutral red uptake assay (NR, data displayed in red), and 3-(4,5-dimethylthiazol-2-yl)-2,5-diphenyltetrazolium reduction assay (MTT, data displayed in purple), as indirect measures of cell viability. Data are presented as percentage of cell death relative to the negative controls and are from four independent experiments performed in triplicate. Curves were fitted to the dosimetric logit model (parameters displayed in Table 1). The dotted lines are the upper and lower limits of the 95% confidence interval of the best estimate of mean responses. The dashed grey lines represent 50% and 100% effect (color figure online)

Cytochrome P450 (CYP450) metabolism impacts hepatotoxicity elicited by 3-methylmethcathinone (3-MMC)

To estimate the role of the main CYP450 enzymes involved in the metabolism of phenethylamines in the hepatotoxicity caused by 3-MMC, primary hepatocytes were incubated with specific inhibitors of different isoforms, namely CYP2D6, CYP2E1 and CYP3A4; a general inhibitor of CYP450 was additionally used. The results obtained are represented in Fig. 2 and Table 1.

When CYP2D6 was inhibited, significantly higher 3-MMC concentrations were needed to induce similar levels of cell death (EC_{50} 2.08 mM), compared to the non-inhibited cells (EC_{50} 1.68 mM). When the cells were pre-treated with metyrapone (CYP2E1 inhibitor), the concentration–response curve of 3-MMC was shifted to the right (EC_{50} 1.40 mM), at 3-MMC concentrations up to ~ 1.20 mM, indicating lower toxicity upon metabolic CYP2E1 inhibition at low concentrations. Nevertheless, at higher 3-MMC concentrations, the inhibition of CYP2E1 increased cell death. Inhibition of CYP3A4 did not influence 3-MMC toxicity. The CYP450 general inhibition only increased cell death from ~ 1.03 mM 3-MMC on (EC_{50} 1.71 mM).

To clarify the role of 3-MMC metabolism by CYP450 on the observed effects, two concentrations from the low cytotoxic range (less than 15% cell death) were selected (i.e.

Table 1 Estimated parameters for the logit model (best-fit regression) of 3-methylmethcathinone (3-MMC) in the different viability assays, after 24-h incubation of primary rat hepatocytes, at 37 °C, in the presence or absence of different isoforms of cytochrome P450 (CYP) inhibitors

Assay	CYP inhibitor	Parameters for the logit regression model			EC_{50} (mM)	NOEC (mM)	LOEC (mM)	*p* value
		θ_1^a	θ_2^b	θ_{max}^c				
MTT	No inhibitor	−1.65	7.14	101.40	1.68	0.38	0.53	–
	CYP 3A4	−1.69	6.93	103.70	1.71	0.53	0.64	$p=0.9758$ (vs. no inhibitor)
	CYP 2E1	−2.36	16.70	96.08	1.40	0.74	1.04	$p=0.0031$ (vs. no inhibitor)
	CYP 2D6	−3.19	10.15	97.96	2.08	1.04	1.25	$p=0.0005$ (vs. no inhibitor)
	CYP 450	−1.68	10.00	101.30	1.46	0.74	1.04	$p=0.0288$ (vs. no inhibitor)
LDH	No inhibitor	−4.44	8.96	100.20	3.13	1.04	1.31	$p<0.0001$ (vs. MTT no inhibitor)
NR	No inhibitor	−0.93	6.62	102.30	1.36	0.31	0.38	$p=0.0061$ (vs. MTT no inhibitor); $p<0.0001$ (vs. LDH no inhibitor)

Metyrapone at 500 µM was used as specific inhibitor of the isoform CYP2E1; quinidine at 10 µM was used as specific inhibitor of the isoform CYP2D6; ketoconazole at 1 µM was used as specific inhibitor of the isoform CYP3A4; and 1-aminobenzotriazole (ABT) at 1 mM was used as general inhibitor of CYP450

CYP cytochrome P450, *EC50* concentration of 3-MMC that induces half-maximal response, i.e. 50% effect, in the respective assay, *NOEC* no observed effect concentration, *LOEC* lower observed effect concentration, *MTT* 3-(4,5-dimethylthiazol-2-yl)-2,5-diphenyltetrazolium, *LDH* lactate dehydrogenase, *NR* neutral red

[a]Location parameter

[b]Slope parameter

[c]Maximal effect, expressed as % cell death (data scaled between 0 and 100% cell death, corresponding to negative controls and positive controls, respectively). Comparisons between curves (θ_{max}, θ_1 and θ_2) were performed using the extra sum-of-squares *F* test. *p* values lower than 0.05 were considered statistically significant

0.8 mM and 1 mM) for the evaluation of 3-MMC metabolic rate, when cells were incubated with inhibitors of CYP450 isoforms. These concentration levels are in line with those used in similar studies for amphetamines (Dias da Silva et al. 2013a, 2017; Pontes et al. 2010). Of note, selective inhibition of CYP2D6 and CYP2E1 resulted in an increase of overall biotransformation of 3-MMC ($p<0.05$), while general P450 inhibition and inhibition of CYP3A4 decrease the amount of 3-MMC metabolised ($p<0.05$). In the absence of CYP inhibition, the metabolism of 3-MMC slightly increased with the drug concentration ($p<0.05$).

3-Methylmethcathinone (3-MMC) increases intracellular oxidative stress

As represented in Fig. 3, ROS and RNS production following exposure of hepatocytes to 3-MMC increased with increasing concentrations of the drug. Although at 1 µM, 3-MMC already induced an increase in ROS/RNS levels by 25%, this augment only presented statistical significance ($p<0.05$) when 3-MMC was present at higher concentrations (≥ 10 µM).

Glutathione is an important antioxidant that prevents cell damage induced by ROS/RNS. Therefore, the evaluation of GSH and GSSG levels in primary rat hepatocytes exposed to 3-MMC was used to provide complementary information on the redox cell status. As depicted in Fig. 4, the increase in the ROS and RNS production is consistent with the GSH depletion observed herein. Accordingly, the results from our study indicate that a significant decline in GSH was observed for all concentrations of 3-MMC tested ($p<0.01$), with the exception of 10 µM.

On the contrary, there were no significant alterations in the intracellular levels of oxidised glutathione, compared to the control incubations (4.59 ± 0.26 nmol GSSG/mg protein), except for 3-MMC at 500 µM that induced an increase in GSSG to 8.24 ± 1.93 nmol GSSG/mg protein (Fig. 4, $p<0.05$). These results were consistent with the significant decrease of GSH/GSSG ratios after cell incubations with the drug (Fig. 4, $p<0.0001$).

3-Methylmethcathinone (3-MMC) does not alter mitochondrial membrane potential but compromises cell energetic status

Mitochondrial membrane potential was not affected by 3-MMC (data not shown), but, cellular ATP levels significantly decreased at concentrations ≥ 100 µM (Fig. 5, $p<0.05$).

3-Methylmethcathinone (3-MMC) activates intrinsic, extrinsic and common apoptotic pathways

The caspase-3, -8 and -9 activities were evaluated after hepatocyte exposure to 3-MMC and the results are presented

in Fig. 6. The activity of the three caspases was maximal when cells were treated with 10 µM of 3-MMC. At this concentration level, caspase-3 activity almost duplicated (189.2 ± 21.9; % $p < 0.05$), while caspase-8 (148.1 ± 13.8%; $p < 0.01$) and caspase-9 (155.3 ± 13.5%; $p < 0.01$) activities were approximately 50% higher than control activity. At higher concentrations (100 µM and 500 µM) caspases activity suffered a drastic decrease to levels close to controls.

These results were compatible with alterations of the nuclear morphology, which suggest induction of apoptosis at 1 µM (Fig. 7b), as depicted by the pyknotic nuclei labelled by Hoechst 33342 (early apoptosis; highlighted with green arrows) or by the red condensed nuclei stained by PI (late apoptotic cells; highlighted with orange arrows). The highest late apoptotic levels occurred at 10 µM (Fig. 7c) and 100 µM (Fig. 7d). At the highest concentrations, necrosis predominates, as indicated by the red large nuclei (highlighted with red arrows in Fig. 7d at 100 µM; and Fig. 7e at 500 µM). Control cells (Fig. 7a) display nuclei with regular contours and have a large and round size.

3-Methylmethcathinone (3-MMC) induces increase of acidic vesicular organelles (AVOs) compatible with autophagy in primary hepatocytes

3-MMC elicited a significant concentration-dependent increase of AO-stained AVOs compatible with autophagosomes (pre-autophagosomes, autophagosomes, and autolysosomes), which became particularly evident at 100 µM and 500 µM (Fig. 8).

Discussion

Over the last few years, 3-MMC has been deemed responsible for several fatal and non-fatal intoxications (Adamowicz et al. 2014, 2016; Ameline et al. 2018; Backberg et al. 2015; Ferreira et al. 2019; Jamey et al. 2016; Sande 2016). As a structural isomer of the popular drug mephedrone, 3-MMC has psychostimulant properties similar to amphetamines and strikingly resembles the pharmacological and toxicological symptoms of the naturally occurring analogue cathinone, in humans (Ferreira et al. 2019). With the increase in consumption and the lack of studies on 3-MMC, its toxicological assessment became mandatory. Since the liver is one of the most affected organs by the toxicity of amphetamine-like drugs (Dias da Silva et al. 2013a, b) and cathinone derivatives (Araujo et al. 2015; Valente et al. 2016a, b), including mephedrone (James et al. 2011; Joanna et al. 2017; Kasick et al. 2012; Schifano et al. 2012; Tarkowski et al. 2018), we herein conducted a pioneer investigation on the deleterious effects of 3-MMC in primary hepatocytes. Primary cultures are still considered the most suitable model for the toxicological screening of new drugs, for investigating the induction of CYPs by chemical inducers, and for the establishment of the metabolic profiles of xenobiotics (Chen et al. 2017; Dias da Silva et al. 2017).

The herein reported hepatocyte damage directly increased with the concentration of 3-MMC in all cell viability assessments, yet the 3-MMC potency was different among the different tests, providing information about the relative sensitivity of target organelles when exposed to the drug. Our data suggest that toxicological effects were perceived in lysosomes at lower concentrations, followed by mitochondria and finally the cytoplasmic membrane. By comparison with data available in the literature, 3-MMC is generally less damaging to mitochondria than most cathinones and other substituted amphetamines. In spite of the apparent closely related chemical structure, the toxicities of 4-MEC (MTT EC_{50} 835 µM), and also of MDPV (MTT EC_{50} 756 µM) and pentedrone (MTT EC_{50} 650 µM) were significantly higher than that of 3-MMC (MTT EC_{50} 1.68 mM) in the same in vitro settings (Valente et al. 2016a), but were in line with the reported toxicities for methylone (MTT EC_{50} 1.26 mM), MDMA (MTT EC_{50} 1.07–2.50 mM) and amphetamine (MTT EC_{50} 1.87 mM) (Dias da Silva et al. 2013b; Valente et al. 2016a). Also, the damage caused by 3-MMC to the cytoplasmic membrane (LDH EC_{50} 3.13 mM) was lower than that provoked by MDPV (LDH EC_{50} 2.06) and MDMA (LDH EC_{50} 1.99 mM), but in agreement with that reported for methylone (LDH EC_{50} 3.20 mM) in dopaminergic SH-SY5Y neuron-like cells (Valente et al. 2017b). No information on the damage induced by cathinones to the lysosome is available in the literature for the sake of comparison, however, amphetamine induced no significant differences in the amount of NR retained by primary rat heart cells treated for 24 h with drug concentrations up to 1 mM (Melchert and Welder 1992); and also no effects higher than 10% were observed in HepG2 hepatoma immortalised cells exposed to four amphetamine designer drugs (concentrations varying from 500 µM to 3 mM) at similar incubation conditions (Dias da Silva et al. 2013a).

The study of the pharmacokinetic profile of 3-MMC in pigs (Shimshoni et al. 2015) showed a low bioavailability after oral administration that was similar to that reported for mephedrone in rats (7%) and suggests that this drug suffers an extensive first-pass metabolism. The biotransformation of 3-MMC may result in metabolites displaying different toxicological potencies and, therefore, variations on the expression of enzymes that catalyse specific metabolic pathways may be important predisposing factors for toxicity. Regarding the contribution of metabolism by cytochrome P450 isoforms to the 3-MMC-induced hepatotoxicity, CYP2E1 and CY2D6 seem to mediate a possible toxification of the drug at physiologically relevant concentrations (< 1.3 mM), as evidenced by the decrease in toxicity when

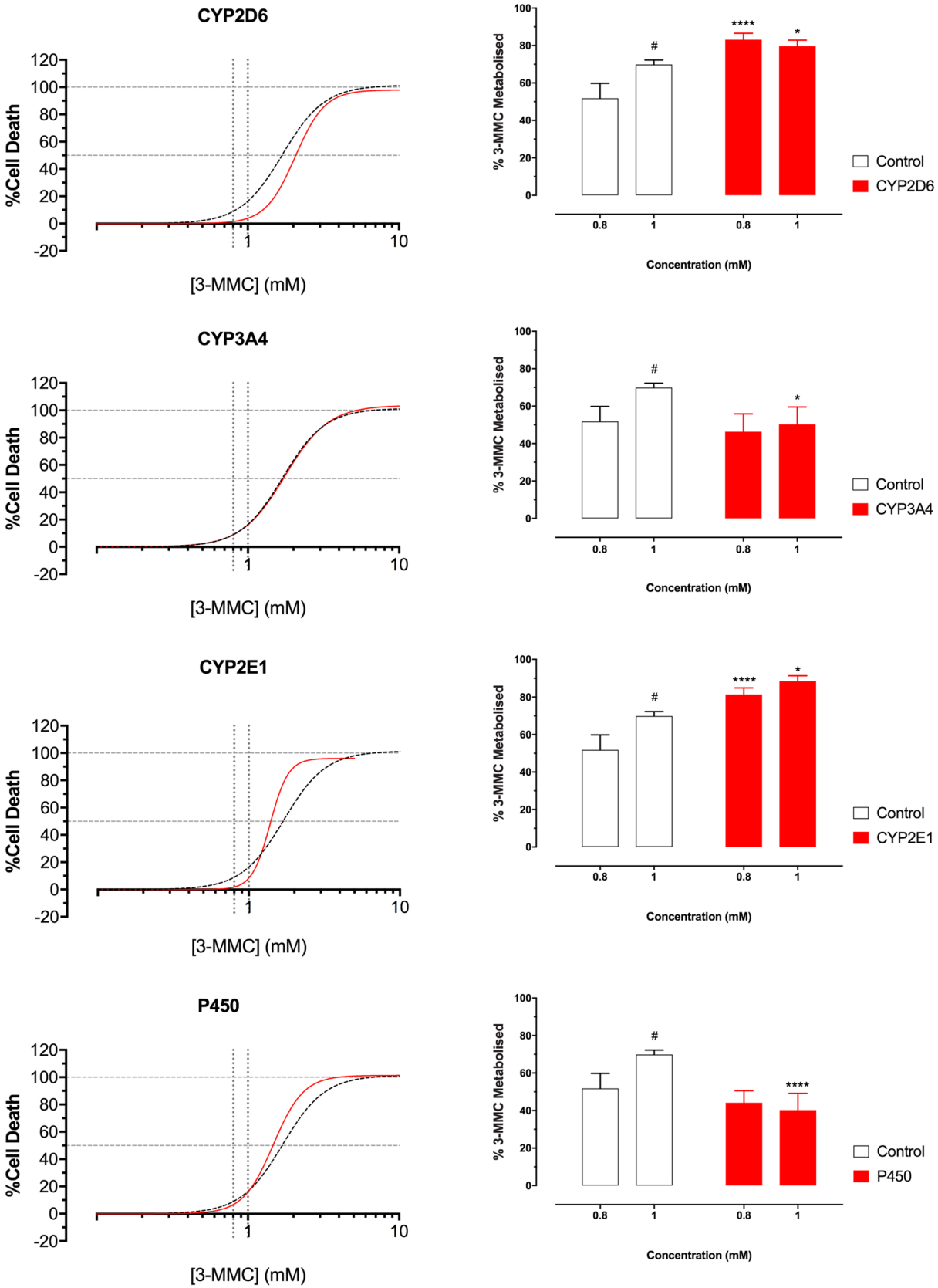
CYP2D6
%Cell Death
[3-MMC] (mM)
% 3-MMC Metabolised
Concentration (mM)
Control
CYP2D6
CYP3A4
Control
CYP3A4
CYP2E1
Control
CYP2E1
P450
Control
P450

◂**Fig. 2** Left side: cell death obtained in the 3-(4,5-dimethylthiazol-2-yl)-2,5-diphenyltetrazolium (MTT) reduction assay, as an indirect measure of cell viability, after 24-h exposures at 37 °C of primary rat hepatocytes to 3-methylmethcathinone (3-MMC), in the presence (red solid curves) or absence (black dashed curves) of different inhibitors of cytochrome P450 isoforms (CYP). Data are presented as percentage of cell death relative to the negative controls and are from four independent experiments performed in six replicates. Curves were fitted to the dosimetric logit model (parameters displayed in Table 1). The dashed grey lines represent 50% and 100% effect. Right side: metabolism of 3-MMC determined by GC–MS when tested at 800 µM or 1 mM, in the presence (red bars) or absence (white bars) of P450 specific and non-specific inhibitors. Data are mean ± standard error of the mean (SEM) and were obtained from four independent experiments run in duplicate. Metyrapone was used as inhibitor of the isoform CYP2E1; quinidine was used as inhibitor of the isoform CYP2D6; ketoconazole was used as inhibitor of the isoform CYP3A4; and 1-aminobenzotriazole (ABT) was used as general inhibitor of cytochrome P450. Statistical comparisons were made using one-way ANOVA/Dunnett's post hoc test. $^{*}p<0.05$; $^{****}p<0.0001$, vs. control at the same concentration; $^{\#}p<0.05$, vs. control at 800 µM (color figure online)

these enzymes were inhibited. This fact might be of particular consequence for 3-MMC as a relevant toxicokinetic expectation stems from the occurrence of drug–drug interactions with often co-administered substances that are also metabolised by CYP450 (Adamowicz et al. 2014; Ferreira et al. 2019; Jamey et al. 2016). CYP2D6-mediated bioactivation is an effect well acknowledged for MDMA (da Silva et al. 2014b; Perfetti et al. 2009), although the formation of highly unstable redox active orthoquinones is not anticipated from the molecular structure of 3-MMC due to the absence of the methylenedioxy moiety. Analysis of a hair sample obtained from an individual charged by drug dealing revealed metabolism of 3-MMC into 3-methylephedrine and 3-methylnorephedrine (Frison et al. 2016), but toxicological information for these substances is absent. To the best of our knowledge, there is no further information regarding 3-MMC metabolism but, based on the structures of these metabolites, one could speculate metabolic pathways similar to those of mephedrone (β-keto-reduction followed by *N*-demethylation). While in vitro studies suggest that mephedrone phase I metabolism is mainly regulated by CYP2D6 (Pedersen et al. 2013b), a potential role for CYP2D6 in the β-keto reduction of cathinone to phenylpropanolamine in humans has also been argued, since urinary ratios parent drug/metabolite were significantly correlated with CYP2D6 genotype and with the CYP2D6 metabolic ratio (Bedada et al. 2015, 2018). Accordingly, Papaseit et al. (2016) suggested that polymorphisms in this isoform, as well as drug competition or inhibition by other co-administered drugs, would increase potential risk of toxicity. On the other hand, 3-MMC itself might be implicated in CYP2D6 inhibition, as observed for its nor-3-demethylated counterpart cathinone. In fact, studies with Ethiopian male volunteers after 1 week of daily use of 400 g fresh Khat leaves, established that cathinone was both a substrate and competitive inhibitor of CYP2D6 (Bedada et al. 2015, 2018). Although quantification and toxicological evaluation of the metabolites of 3-MMC are beyond the scope of this study, since we obtained increased 3-MMC metabolic rates following inhibition of CYP2D6 and CYP2E1 isoforms, we hypothesised that the drug enters in alternative metabolic pathways that, although less specific, more rapidly degrade 3-MMC than its CYP2D6 and CYP2E1 counterparts; and that the biotransformation of the drug through these routes may result in metabolites with lower toxicity. In accordance, P450 function is highly redundant and when CYP2D6 or CYP2E1 are inhibited, for example by competition with other substances, drugs such as 3-MMC undergo biotransformation through alternative pathways (Zanger and Schwab 2013). An example of such an enzyme is CYP3A4, which has a major role in the detoxification of several drugs (Zanger and Schwab 2013). Our data indicate that specific inhibition of CYP3A4 at physiologically relevant 3-MMC concentrations, and also overall inhibition of P450, produced toxicities undistinguishable from the non-inhibited cells, although significantly reducing the metabolic transformation of 3-MMC. This might indicate that biotransformation of 3-MMC by CYP450 alternative pathways result in metabolites with similar toxicity to the parent drug.

Cytochrome P450 metabolism is a relevant source of oxidant species in vivo, only supplanted by the mitochondrial aerobic respiration. A drug-induced rise in the burden of reactive species causes the decrease of antioxidant protection and will ultimately result in failure to repair oxidative damage. The formation of ROS/RNS is one of the mechanisms responsible for the toxicity of amphetamines in primary rat hepatocytes (da Silva et al. 2014a) and it was also reported for other cathinones, although at higher concentrations. Valente et al. (2016a) showed that 4-MEC induced a significant increase in oxidative stress at concentrations higher than 400 µM, and similar levels of disturbance in production of ROS/RNS occurred for MDMA at 1 mM in the same model (da Silva et al. 2014a). Recently, the prooxidative effects of mephedrone were also confirmed in the liver of animals exposed for 1 h at doses higher than 5 mg/kg (Tarkowski et al. 2018) by the increase of malondialdehyde, the main by-product of lipid peroxidation. Results from our study indicate that ROS and RNS production was dependent on 3-MMC concentration, starting at 10 µM, and although no rescue experiments were herein conducted with antioxidants to provide further insights into the mechanisms of the elicited oxidative stress, it was previously demonstrated that *N*-acetyl-L-cysteine and vitamin C partially reverted cell death induced by other cathinone derivatives in primary rat hepatocytes (Valente et al. 2016a).

In addition to increased prooxidant species levels, events reflecting antioxidant depletion have also been considered

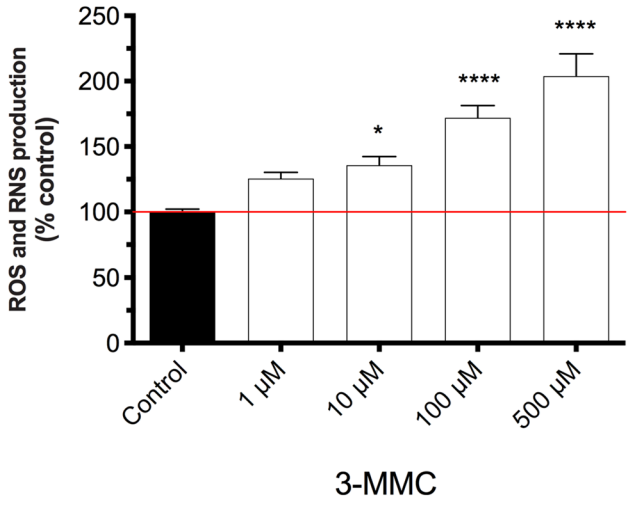

Fig. 3 Production of oxygen and nitrogen reactive species (ROS and RNS), measured through the 2′,7′-dichlorofluorescin diacetate (DCFH-DA) assay, in rat primary hepatocytes after 24-h incubation with 3-methylmethcathinone (3-MMC), at 37 °C. Results are expressed as percentage control ± standard error of the mean (SEM) from four independent experiments, run in six replicates. Statistical comparisons were made using one-way ANOVA/Dunnett's post hoc test. *$p < 0.05$; ****$p < 0.0001$, vs. control

as potential biomarkers of drug-induced hepatotoxicity. Glutathione is an important non-enzymatic antioxidant cell defence, preventing cell damage induced by ROS/RNS, and therefore, the evaluation of the GSH and GSSG levels in hepatocytes exposed to 3-MMC was used to provide complementary information on the redox status of hepatocytes. A decline in GSH was observed for all concentrations of 3-MMC, with the exception of 10 µM. This might mean that, at this concentration, the cell is trying to respond to the drug insult by activating pro-survival mechanisms. At higher concentrations, however, the capacity of cell response was most likely exceeded as a decline in the GSH intracellular content was observed. Cells exposed to sustained oxidative stress accumulate GSSG with reduction of the GSH/GSSG ratio. Some compounds, such as MDMA, MDA, methylone and MDPV, can suffer extensive hepatic metabolism into catechols and be further oxidised to very unstable orthoquinones (Carvalho et al. 2004; Pedersen et al. 2013a; Strano-Rossi et al. 2010). When glutathione is conjugated with these orthoquinones, it produces glutathione-*S*-yl-adducts, which are still redox active and thus can be readily oxidised and further reduced by a second molecule of glutathione, resulting in 2,5-bis-(glutathione-*S*-yl)-conjugates. Formation of such conjugates might justify the discrepancies observed regarding the decrease of GSH, which was not compensated by the GSSG increase. Despite the lack of evidence suggesting that the molecule of 3-MMC can be transformed into catechols, disruption of thiol redox homeostasis may involve other reactive metabolites and/or mechanisms of impairment of the regulation of glutathione, such as the impairment of glutathione peroxidase/reductase (GSH-Px/GSSG-Rd) enzyme system. In accordance, incubation of freshly isolated rat hepatocytes with d-amphetamine (at concentrations as low as 80 µM) revealed the presence of the (glutathion-*S*-yl)-*p*-hydroxyamphetamine, whose formation was prevented by pre-treatment of hepatocytes with the P450 inhibitors (Carvalho et al. 1996). A similar p-hydroxy glutathione adduct might be hypothesised for 3-MMC. Also, GSH-Px, superoxide dismutase and catalase were overexpressed in the frontal cortex of Swiss-CD1 mice following administration of mephedrone (Ciudad-Roberts et al. 2016).

The impairment of cell redox state and the compromise of antioxidant mechanisms might result in severe detrimental effects through the production of peroxides and free radicals that damage all cellular components, including biomolecules (proteins, lipids, and DNA) and organelles. In this regard, mitochondria act like cell powerhouses by generating energy and their integrity is very important also

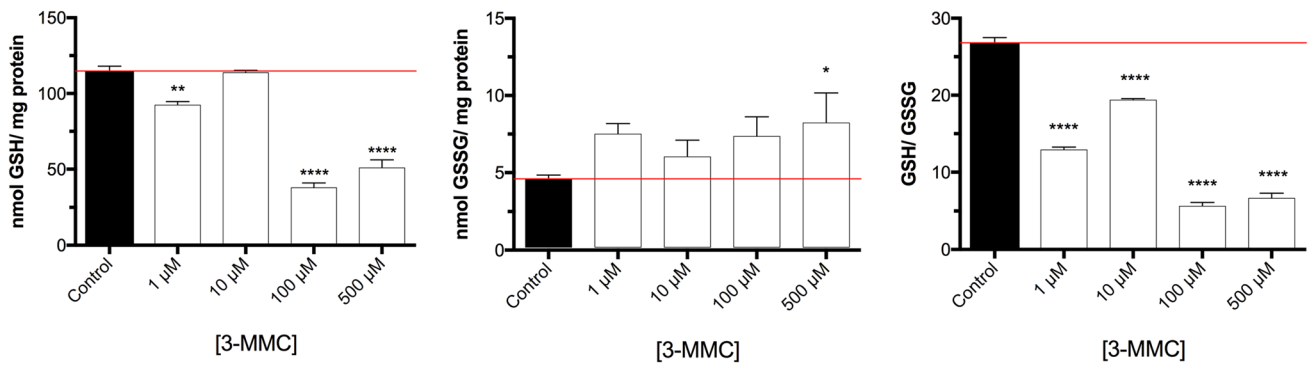

Fig. 4 Intracellular contents of reduced (GSH) and oxidised glutathione (GSSG), and intracellular GSH/GSSG ratio in rat primary hepatocytes after 24-h incubation with 3-methylmethcathinone (3-MMC), at 37 °C. Results are expressed as mean ± standard error from the mean (SEM) from four independent experiments. Statistical comparisons were made using one-way ANOVA/Dunnett's post hoc test. *$p < 0.05$; **$p < 0.01$; ****$p < 0.0001$, vs. control

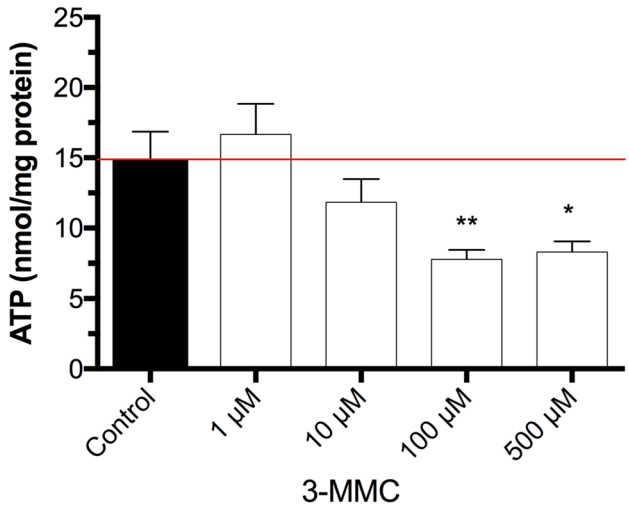

Fig. 5 Intracellular ATP levels in primary rat hepatocytes after 24-h incubation with 3-methylmethcathinone (3-MMC), at 37 °C. Results are expressed as mean ± standard error of the mean (SEM) from four independent experiments. Statistical comparisons were made using one-way ANOVA/Dunnett's. *$p < 0.05$; **$p < 0.01$, vs. control

to propagate death signals from the inside or outside the cell. The induction of the stress signalling pathways JNK/SAPK triggers cytochrome *c* release from mitochondria and activation of apoptosome, cleaving the pro-enzyme caspase-9 into its active form. This in turn cleaves downstream executioner procaspase-3, procaspase-6 and procaspase-7, which activate the propagation of the apoptotic cascade, leading to the cleavage of intracellular substrates and to morphological and biochemical changes that culminate in cell death (Dias da Silva et al. 2013a). Cell death stimuli might also be originated from the exterior of the cell following drug-induced injury, as observed for Khat in acute myeloid leukemia cells (Bredholt et al. 2009). In this regard, activation of the extrinsic apoptotic pathway through the cleavage of procaspase-8 also induces activation of the common apoptotic pathway through the binding of a pro-apoptotic ligand to the cell death receptor. Although 3-MMC did not promote a significant depolarisation of mitochondria, activation of apoptosis was confirmed in our study by cell nuclear morphology and caspase activation. Maintenance of mitochondrial membrane potential is tightly related to several mitochondrial processes, including ATP synthesis. When cells were treated with 1 µM of 3-MMC, ATP levels were slightly higher than those of the control, again supporting energy-dependent pro-survival mechanisms. ATP is essential to execute many energy-requiring processes, such as apoptosis. Of note, the intracellular energetic impairment was only significant at concentrations above 10 µM, which could justify the absence of caspases activation at this concentration level, since apoptosis involves a number of ATP-dependent processes. The caspase-3, caspase-8 and caspase-9 activities were maximal when cells were treated with 10 µM 3-MMC; a much lower concentration than that observed for 4-MEC (1.6 mM) in the same cell model (Valente et al. 2016a). At higher concentrations, caspase activities suffered a drastic decrease to levels close to controls. This was also concomitant with a significant depletion of cell energetic stores and GSH, and increased formation of ROS and RNS, suggesting that the hepatotoxicity observed at these concentration levels must follow other forms of cell death, such as necrosis and autophagy. Autophagy is tightly interconnected with metabolic networks and redox balance, as it contributes to the reutilisation of the cell's own constituents for energy, by interacting with lipid and carbohydrate metabolism (Singh and Cuervo 2011); and also to the removal of altered or dysfunctional biomolecules, such as irreversibly oxidised proteins, DNA and lipids (Filomeni et al. 2015). Therefore, increased reactive species, thiol redox state imbalance and low energetic homeostasis may all represent important mediators of autophagy. Coherently, our data indicate a 3-MMC concentration-dependent increase of acidic vesicular organelles, which are consistent with the

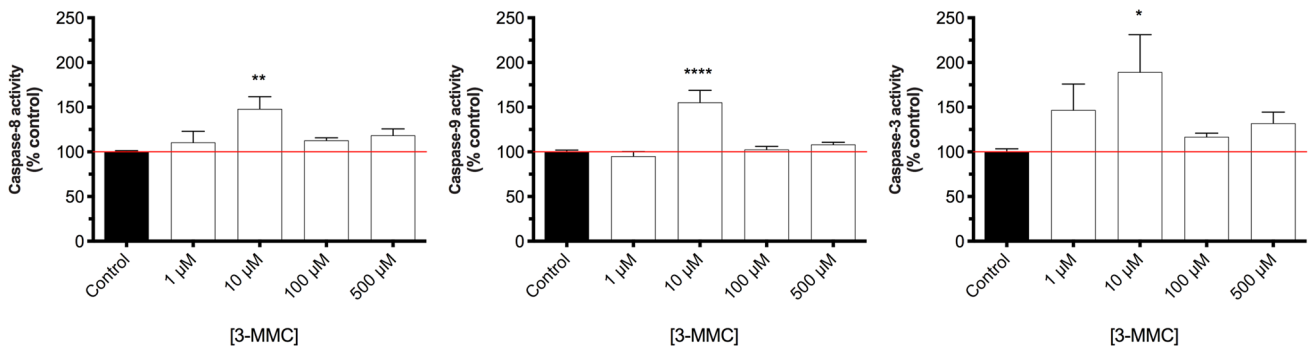

Fig. 6 Caspase-3, -8, and -9 activities in primary rat hepatocytes after 24-h incubations with 3-methylmethcathinone (3-MMC), at 37 °C. Results are expressed as percentage of control ± standard error of the mean (SEM) from four independent experiments. Statistical comparisons were made using one-way ANOVA/Dunnett's post hoc test. *$p < 0.05$; **$p < 0.01$; ****$p < 0.0001$, vs. control

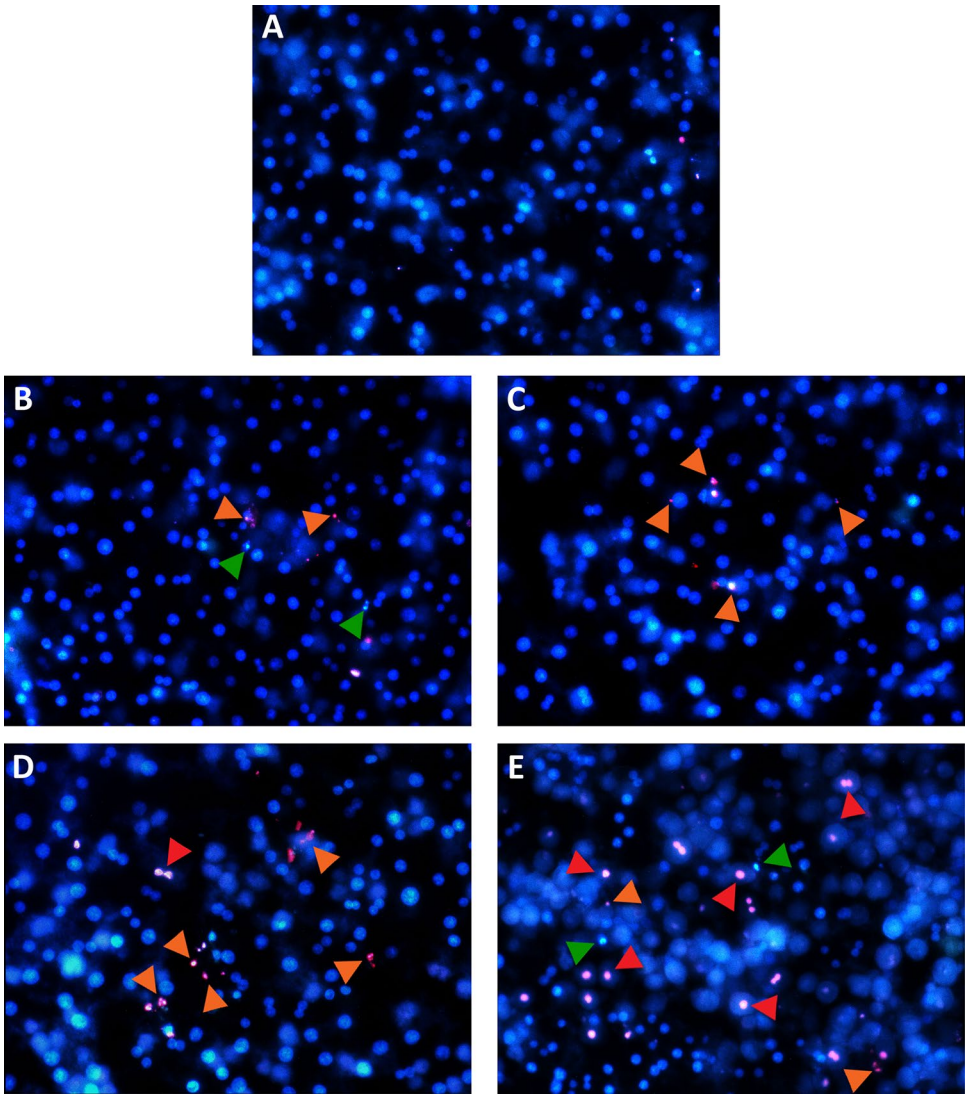

Fig. 7 Hoechst 33342/propidium iodide staining of primary rat hepatocytes after exposure to control cells (**a**) or 3-methylmethcathinone (3-MMC) at 1 µM (**b**), 10 µM (**c**), 100 µM (**d**) and 500 µM (**e**) for 24 h, at 37 °C. Red arrows indicate necrotic cells, green arrows indicate early apoptotic cells and orange arrows indicate late apoptotic cells. Original magnification, ×200 (color figure online)

formation of autophagosomes. Although peremptory confirmation of autophagy would demand verification of specific markers of the process, this is in line with data reported for 3-fluoromethcathinone (3-FMC) in HT22 cells (Siedlecka-Kroplewska et al. 2018), for α-pyrrolidinononanophenone in SK-N-SH cells (Matsunaga et al. 2017) and for methylone and MDPV in dopaminergic SH-SY5Y cells (Valente et al. 2017a). In these studies on neuronal models, the authors observed the oxidative stress-dependent conversion of cytosolic LC3-I to membrane-bound LC3-II (Matsunaga et al. 2017; Siedlecka-Kroplewska et al. 2018; Valente et al. 2017a). Additionally, the level of p62/SQSTM1 protein decreased after treatment with 3-FMC (Siedlecka-Kroplewska et al. 2018). Our data evidenced for the first time the formation of autophagic vacuoles in hepatocytes after exposure to 3-MMC.

Contrary to autophagy and apoptosis, cell death by necrosis follows an unregulated sequence of events involving severe cell damage, as the aggressive nature of the injury offers the cell no means to program its suicide. The increase in 3-MMC concentration might be sufficient to provide cells with such stimuli, as denoted by cell morphological alterations at 500 µM. Necrotic phenomena were previously described following intravascular abuse of mephedrone (Frances et al. 2018) and related cathinones (Nanavati and Herlitz 2017; Saleh et al. 2016).

All the assays performed herein to elucidate the mechanisms responsible for the observed hepatotoxicity were conducted at 3-MMC concentrations ranging between 1 and 500 µM, which is in line with the values described in clinical and/or forensic cases. Accordingly, a mean blood concentration of 1.6 µg/mL (~9.03 µM) was found for 95 individuals intoxicated with 3-MMC (Adamowicz et al. 2016). Also, blood concentrations ranging between 0.29 and 124.16 µM (mean of 15.24 µM, i.e. 2.7 µg/mL) were found from the study of 97 fatalities attributed to mephedrone. In this

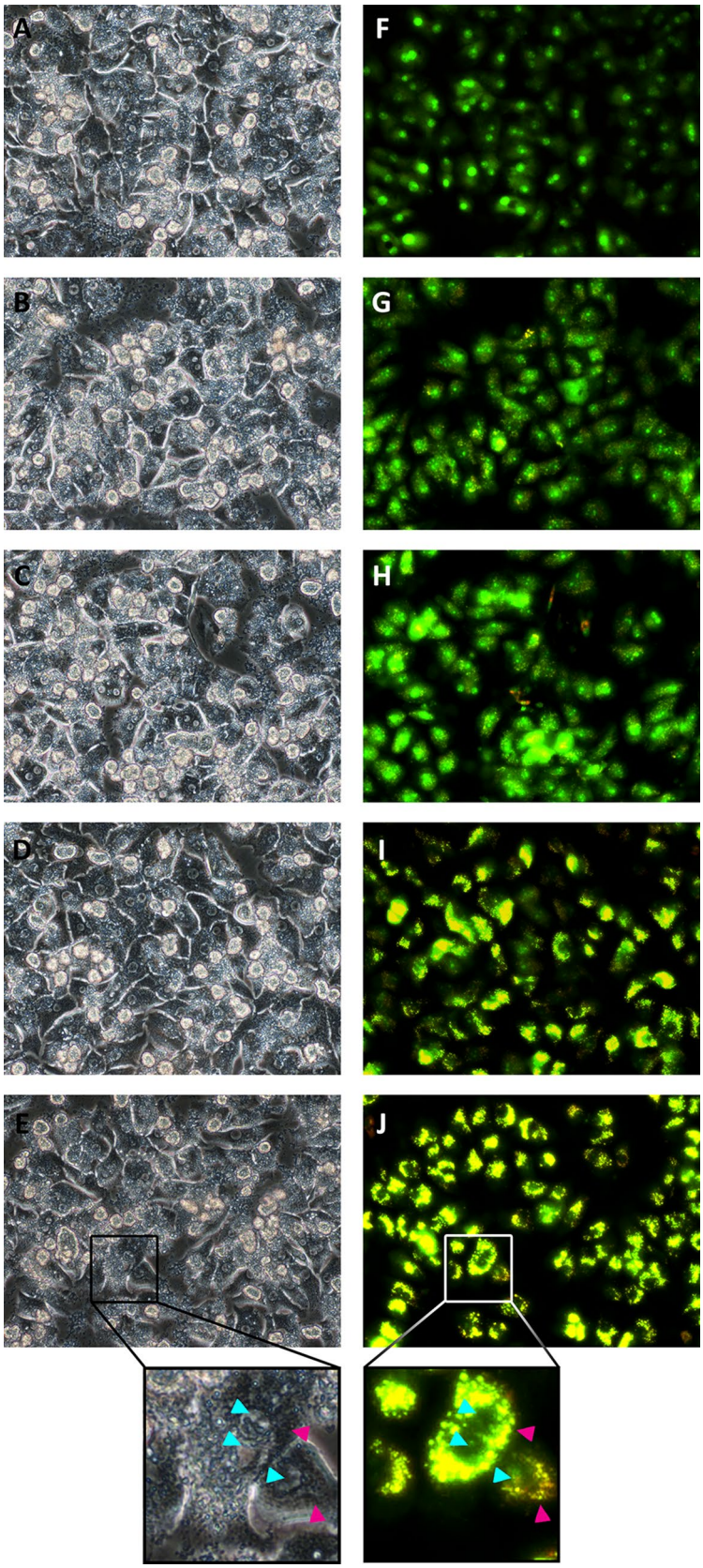

Fig. 8 Representative phase contrast (**a**–**e**) and fluorescence (**f**–**j**) micrographs of primary hepatocytes stained with acridine orange after exposure to 3-methylmethcathinone (3-MMC) for 24 h, at 37 °C. Cells treated with 1 µM (**b**, **g**), 10 µM (**c**, **h**), 100 µM (**d**, **i**) and 500 µM (**e**, **j**) of 3-MMC present acidic vesicular organelles stained in yellow (pink arrow), which are absent in control cells (**a**, **f**). Blue arrows show the nuclei (color figure online)

regard, the realistic concentrations of 10 µM and 100 µM were first chosen to be tested and, in addition, we selected a lower and a higher concentration, the latter with the purpose of elucidating the molecular mechanisms involved, as all too often the in vitro mechanistic pathways observed in vivo for drugs could only be triggered at higher, unrealistic concentrations (Papaseit et al. 2017).

Conclusion

For the first time, the in vitro hepatotoxic effects of 3-MMC have been demonstrated. Drug metabolism through CYP2D6 and CYP2E1 appears to be involved in the toxicological effects of 3-MMC. Future research should aim at quantifying such potentially toxic metabolites as well as describing their putative mechanisms of hepatotoxicity. This synthetic cathinone induced oxidative stress, GSH depletion, increased GSSG, as well as caspase-3, -8, and -9 activation. No significant alterations were observed in the mitochondrial membrane potential ($\Delta\Psi m$), which is important for ATP synthesis, but ATP intracellular content significantly decreased at concentrations higher than 100 µM. Overall, data presented herein allowed us to conclude that at 10 µM 3-MMC, the elicited hepatotoxicity might be triggered both by mitochondria-dependent (intrinsic) and mitochondria-independent (extrinsic) pathways of apoptotic cell death. At higher drug concentrations, other cell death pathways might be at play, such as autophagy and necrosis. The present study is a starting point in the research concerning 3-MMC and, therefore, further investigation is required to elucidate users that should be alert of the risks associated with the abuse of this substance.

Acknowledgements This work received financial support from European Union funds [Fundo Europeu de Desenvolvimento Regional (FEDER)] under the program PT2020 (UID/MULTI/013788/2013) and COMPETE 2020—Operational Program for Competitiveness and Internationalization (POCI), and National funds [Fundação para a Ciência e Tecnologia and Ministério da Educação e Ciência (FCT/MEC)] through the framework of the project POCI-01-0145-FEDER-029584. To all financing sources the authors are greatly indebted.

Compliance with ethical standards

Conflict of interest The authors declare that they have no conflict of interest.

References

ACMD (2010) ACMD report on the consideration of the cathinones by the advisory council on the misuse of drugs (ACMD). http://www.homeoffice.gov.uk/publications/agencies-public-bodies/acmd1/acmd-cathinodes-report-2010?view=Standard&pubID=878838

Adamowicz P (2017) Distinction of constitutional isomers of mephedrone by chromatographic and spectrometric methods AU—Zuba, Dariusz. Aust J Forensic Sci 49(6):637–649. https://doi.org/10.1080/00450618.2016.1167240

Adamowicz P, Zuba D, Byrska B (2014) Fatal intoxication with 3-methyl-*N*-methylcathinone (3-MMC) and 5-(2-aminopropyl) benzofuran (5-APB). Forensic Sci Int 245:126–132. https://doi.org/10.1016/j.forsciint.2014.10.016

Adamowicz P, Gieron J, Gil D, Lechowicz W, Skulska A, Tokarczyk B (2016) 3-Methylmethcathinone–interpretation of blood concentrations based on analysis of 95 cases. J Anal Toxicol 40(4):272–276. https://doi.org/10.1093/jat/bkw018

Ameline A, Dumestre-Toulet V, Raul JS, Kintz P (2018) Determination of a threshold fatal 3-MMC concentration in human: mission impossible. Psychopharmacology. https://doi.org/10.1007/s00213-018-4941-5

Araujo AM, Valente MJ, Carvalho M et al (2015) Raising awareness of new psychoactive substances: chemical analysis and in vitro toxicity screening of 'legal high' packages containing synthetic cathinones. Arch Toxicol 89(5):757–771. https://doi.org/10.1007/s00204-014-1278-7

Arbo MD, Silva R, Barbosa DJ et al (2014) Piperazine designer drugs induce toxicity in cardiomyoblast h9c2 cells through mitochondrial impairment. Toxicol Lett 229(1):178–189. https://doi.org/10.1016/j.toxlet.2014.06.031

Backberg M, Lindeman E, Beck O, Helander A (2015) Characteristics of analytically confirmed 3-MMC-related intoxications from the Swedish STRIDA project. Clin Toxicol 53(1):46–53. https://doi.org/10.3109/15563650.2014.981823

Bedada W, de Andres F, Engidawork E et al (2015) The psychostimulant khat (*Catha edulis*) inhibits CYP2D6 enzyme activity in humans. J Clin Psychopharmacol 35(6):694–699. https://doi.org/10.1097/JCP.0000000000000413

Bedada W, de Andres F, Engidawork E, Hussein J, LLerena A, Aklillu E (2018) Effects of Khat (*Catha edulis*) use on catalytic activities of major drug-metabolizing cytochrome P450 enzymes and implication of pharmacogenetic variations. Sci Rep 8(1):12726. https://doi.org/10.1038/s41598-018-31191-1

Bluelight (2012) 3-MMC (3-Methylmethcathinone) Megathread. http://www.bluelight.org/vb/threads/608696-3-MMC-(3-Methylmethcathinone)-Megathread-(v1). Accessed 29 Jan 2018

Bredholt T, Dimba EA, Hagland HR et al (2009) Camptothecin and khat (*Catha edulis* Forsk.) induced distinct cell death phenotypes involving modulation of c-FLIPL, Mcl-1, procaspase-8 and mitochondrial function in acute myeloid leukemia cell lines. Mol Cancer 8:101. https://doi.org/10.1186/1476-4598-8-101

Carvalho F, Remiao F, Amado F, Domingues P, Correia AJ, Bastos ML (1996) d-Amphetamine interaction with glutathione in freshly isolated rat hepatocytes. Chem Res Toxicol 9(6):1031–1036. https://doi.org/10.1021/tx9501750

Carvalho M, Milhazes N, Remiao F et al (2004) Hepatotoxicity of 3,4-methylenedioxyamphetamine and alpha-methyldopamine in isolated rat hepatocytes: formation of glutathione conjugates. Arch Toxicol 78(1):16–24. https://doi.org/10.1007/s00204-003-0510-7

Chen JJ, Zhang JX, Zhang XQ et al (2017) Effects of diosmetin on nine cytochrome P450 isoforms, UGTs and three drug transporters in vitro. Toxicol Appl Pharmacol 334:1–7. https://doi.org/10.1016/j.taap.2017.08.020

Ciudad-Roberts A, Duart-Castells L, Camarasa J, Pubill D, Escubedo E (2016) The combination of ethanol with mephedrone increases the signs of neurotoxicity and impairs neurogenesis and learning in adolescent CD-1 mice. Toxicol Appl Pharmacol 293:10–20. https://doi.org/10.1016/j.taap.2015.12.019

da Silva DD, Silva E, Carmo H (2014a) Combination effects of amphetamines under hyperthermia—the role played by oxidative stress. J Appl Toxicol 34(6):637–650. https://doi.org/10.1002/jat.2889

da Silva DD, Silva E, Carvalho F, Carmo H (2014b) Mixtures of 3,4-methylenedioxymethamphetamine (ecstasy) and its major human metabolites act additively to induce significant toxicity to liver cells when combined at low, non-cytotoxic concentrations. J Appl Toxicol 34(6):618–627. https://doi.org/10.1002/jat.2885

Dias da Silva D, Carmo H, Lynch A, Silva E (2013a) An insight into the hepatocellular death induced by amphetamines, individually and in combination: the involvement of necrosis and apoptosis. Arch Toxicol 87(12):2165–2185. https://doi.org/10.1007/s00204-013-1082-9

Dias da Silva D, Silva E, Carmo H (2013b) Cytotoxic effects of amphetamine mixtures in primary hepatocytes are severely aggravated under hyperthermic conditions. Toxicol In Vitro Int J Publ Assoc BIBRA 27(6):1670–1678. https://doi.org/10.1016/j.tiv.2013.04.010

Dias da Silva D, Silva MJ, Moreira P et al (2017) In vitro hepatotoxicity of 'Legal X': the combination of 1-benzylpiperazine (BZP) and 1-(m-trifluoromethylphenyl)piperazine (TFMPP) triggers oxidative stress, mitochondrial impairment and apoptosis. Arch Toxicol 91(3):1413–1430. https://doi.org/10.1007/s00204-016-1777-9

Dias-da-Silva D, Arbo MD, Valente MJ, Bastos ML, Carmo H (2015) Hepatotoxicity of piperazine designer drugs: comparison of different in vitro models. Toxicol In Vitro Int J Publ Assoc BIBRA 29(5):987–996. https://doi.org/10.1016/j.tiv.2015.04.001

EMCDDA (2011) Report on the risk assessment of mephedrone in the framework of the Council Decision on new psychoactive substances by the european Monitoring centre for drugs and drug addiction (EMCDDA), Lisbon. http://www.emcdda.europa.eu/risk-assessments/mephedrone_en

Erowid (2013) Any reports with 3-Methylmethcathinone. http://www.erowid.org/experiences/exp.cgi?S1=592&S2=-1&C1=-1&Str. Accessed 29 Jan 2018

Ferreira B, Dias da Silva D, Carvalho F, de Lourdes Bastos M, Carmo H (2019) The novel psychoactive substance 3-methylmethcathinone (3-MMC or metaphedrone): a review. Forensic Sci Int 295:54–63. https://doi.org/10.1016/j.forsciint.2018.11.024

Filomeni G, De Zio D, Cecconi F (2015) Oxidative stress and autophagy: the clash between damage and metabolic needs. Cell Death Differ 22(3):377–388. https://doi.org/10.1038/cdd.2014.150

Frances M, Fuertes V, Casarrubios JM et al (2018) Fingertip necrosis due to intravascular use of mephedrone: a case report. Plast Reconstr Surg Glob Open 6(8):e1906. https://doi.org/10.1097/GOX.0000000000001906

Frison G, Frasson S, Zancanaro F, Tedeschi G, Zamengo L (2016) Detection of 3-methylmethcathinone and its metabolites 3-methylephedrine and 3-methylnorephedrine in pubic hair samples by liquid chromatography-high resolution/high accuracy Orbitrap mass spectrometry. Forensic Sci Int 265:131–137. https://doi.org/10.1016/j.forsciint.2016.01.039

Green AR, King MV, Shortall SE, Fone KC (2014) The preclinical pharmacology of mephedrone; not just MDMA by another name. Br J Pharmacol 171(9):2251–2268. https://doi.org/10.1111/bph.12628

James D, Adams RD, Spears R et al (2011) Clinical characteristics of mephedrone toxicity reported to the U.K. National Poisons Information Service. Emerg Med J 28(8):686–689. https://doi.org/10.1136/emj.2010.096636

Jamey C, Kintz P, Martrille L, Raul JS (2016) Fatal combination with 3-methylmethcathinone (3-MMC) and gamma-hydroxybutyric acid (GHB). J Anal Toxicol 40(7):546–552. https://doi.org/10.1093/jat/bkw058

Joanna L, Sylwia T, Magdalena G et al (2017) Mephedrone exposure in adolescent rats alters the rewarding effect of morphine in adults. Eur J Pharmacol 810:63–69. https://doi.org/10.1016/j.ejphar.2017.06.007

Kasick DP, McKnight CA, Klisovic E (2012) "Bath salt" ingestion leading to severe intoxication delirium: two cases and a brief review of the emergence of mephedrone use. Am J Drug Alcohol Abuse 38(2):176–180. https://doi.org/10.3109/00952990.2011.643999

Lowry OH, Rosebrough NJ, Farr AL, Randall RJ (1951) Protein measurement with the Folin phenol reagent. J Biol Chem 193(1):265–275

Martinez-Clemente J, Lopez-Arnau R, Carbo M, Pubill D, Camarasa J, Escubedo E (2013) Mephedrone pharmacokinetics after intravenous and oral administration in rats: relation to pharmacodynamics. Psychopharmacology 229(2):295–306. https://doi.org/10.1007/s00213-013-3108-7

Martins MJ, Roque Bravo R, Enea M et al (2018) Ethanol addictively enhances the in vitro cardiotoxicity of cocaine through oxidative damage, energetic deregulation, and apoptosis. Arch Toxicol 92(7):2311–2325. https://doi.org/10.1007/s00204-018-2227-7

Matsunaga T, Morikawa Y, Kamata K et al (2017) alpha-Pyrrolidinononanophenone provokes apoptosis of neuronal cells through alterations in antioxidant properties. Toxicology 386:93–102. https://doi.org/10.1016/j.tox.2017.05.017

Melchert RB, Welder AA (1992) The combined effects of cocaine and amphetamine on primary postnatal rat heart cell cultures. Reprod Toxicol 6(6):467–473

Nanavati A, Herlitz LC (2017) Tubulointerstitial injury and drugs of abuse. Adv Chronic Kidney Dis 24(2):80–85. https://doi.org/10.1053/j.ackd.2016.09.008

Papaseit E, Perez-Mana C, Mateus JA et al (2016) Human pharmacology of mephedrone in comparison with MDMA. Neuropsychopharmacology 41(11):2704–2713. https://doi.org/10.1038/npp.2016.75

Papaseit E, Olesti E, de la Torre R, Torrens M, Farre M (2017) Mephedrone concentrations in cases of clinical intoxication. Curr Pharm Des 23(36):5511–5522. https://doi.org/10.2174/1381612823666170704130213

Pedersen AJ, Petersen TH, Linnet K (2013a) In vitro metabolism and pharmacokinetic studies on methylone. Drug Metab Dispos Biol Fate Chem 41(6):1247–1255. https://doi.org/10.1124/dmd.112.050880

Pedersen AJ, Reitzel LA, Johansen SS, Linnet K (2013b) In vitro metabolism studies on mephedrone and analysis of forensic cases. Drug Test Anal 5(6):430–438. https://doi.org/10.1002/dta.1369

Perfetti X, O'Mathuna B, Pizarro N et al (2009) Neurotoxic thioether adducts of 3,4-methylenedioxymethamphetamine identified in human urine after ecstasy ingestion. Drug Metab Dispos Biol Fate Chem 37(7):1448–1455. https://doi.org/10.1124/dmd.108.026393

Pontes H, de Pinho PG, Fernandes E et al (2010) Metabolic interactions between ethanol and MDMA in primary cultured rat hepatocytes. Toxicology 270(2–3):150–157. https://doi.org/10.1016/j.tox.2010.02.010

Romanek K, Stenzel J, Schmoll S et al (2017) Synthetic cathinones in Southern Germany—characteristics of users, substance-patterns, co-ingestions, and complications. Clin Toxicol 55(6):573–578. https://doi.org/10.1080/15563650.2017.1301463

Saleh A, Tittley J, Anand S (2016) Limb-threatening ischemia in a young man with cathinone "Bath Salt" intoxication: a case report. Ann Vasc Surg 36:294e1–294e5. https://doi.org/10.1016/j.avsg.2016.03.025

Sande M (2016) Characteristics of the use of 3-MMC and other new psychoactive drugs in Slovenia, and the perceived problems experienced by users. Int J Drug Policy 27:65–73. https://doi.org/10.1016/j.drugpo.2015.03.005

Schifano F, Corkery J, Ghodse AH (2012) Suspected and confirmed fatalities associated with mephedrone (4-methylmethcathinone,

"meow meow") in the United Kingdom. J Clin Psychopharmacol 32(5):710–714. https://doi.org/10.1097/JCP.0b013e318266c70c

Shimshoni JA, Britzi M, Sobol E, Willenz U, Nutt D, Edery N (2015) 3-Methyl-methcathinone: pharmacokinetic profile evaluation in pigs in relation to pharmacodynamics. J Psychopharmacol 29(6):734–743. https://doi.org/10.1177/0269881115576687

Siedlecka-Kroplewska K, Wronska A, Stasilojc G, Kmiec Z (2018) The designer drug 3-fluoromethcathinone induces oxidative stress and activates autophagy in HT22 neuronal cells. Neurotox Res 34(3):388–400. https://doi.org/10.1007/s12640-018-9898-y

Silva E, Scholze M, Kortenkamp A (2007) Activity of xenoestrogens at nanomolar concentrations in the E-Screen assay. Environ Health Perspect 115(Suppl 1):91–97. https://doi.org/10.1289/ehp.9363

Singh R, Cuervo AM (2011) Autophagy in the cellular energetic balance. Cell Metab 13(5):495–504. https://doi.org/10.1016/j.cmet.2011.04.004

Strano-Rossi S, Cadwallader AB, de la Torre X, Botre F (2010) Toxicological determination and in vitro metabolism of the designer drug methylenedioxypyrovalerone (MDPV) by gas chromatography/mass spectrometry and liquid chromatography/quadrupole time-of-flight mass spectrometry. Rapid Commun Mass Spectrom 24(18):2706–2714. https://doi.org/10.1002/rcm.4692

Tarkowski P, Jankowski K, Budzynska B, Biala G, Boguszewska-Czubara A (2018) Potential pro-oxidative effects of single dose of mephedrone in vital organs of mice. Pharmacol Rep 70(6):1097–1104. https://doi.org/10.1016/j.pharep.2018.05.010

Valente MJ, Guedes de Pinho P, de Lourdes Bastos M, Carvalho F, Carvalho M (2014) Khat and synthetic cathinones: a review. Arch Toxicol 88(1):15–45. https://doi.org/10.1007/s00204-013-1163-9

Valente MJ, Araujo AM, Bastos Mde L et al (2016a) Editor's highlight: characterization of hepatotoxicity mechanisms triggered by designer cathinone drugs (beta-keto amphetamines). Toxicol Sci 153(1):89–102. https://doi.org/10.1093/toxsci/kfw105

Valente MJ, Araujo AM, Silva R et al (2016b) 3,4-Methylenedioxypyrovalerone (MDPV): in vitro mechanisms of hepatotoxicity under normothermic and hyperthermic conditions. Arch Toxicol 90(8):1959–1973. https://doi.org/10.1007/s00204-015-1653-z

Valente MJ, Amaral C, Correia-da-Silva G et al (2017a) Methylone and MDPV activate autophagy in human dopaminergic SH-SY5Y cells: a new insight into the context of beta-keto amphetamines-related neurotoxicity. Arch Toxicol 91(11):3663–3676. https://doi.org/10.1007/s00204-017-1984-z

Valente MJ, Bastos ML, Fernandes E, Carvalho F, Guedes de Pinho P, Carvalho M (2017b) Neurotoxicity of beta-keto amphetamines: deathly mechanisms elicited by methylone and MDPV in human dopaminergic SH-SY5Y cells. ACS Chem Neurosci 8(4):850–859. https://doi.org/10.1021/acschemneuro.6b00421

Zanger UM, Schwab M (2013) Cytochrome P450 enzymes in drug metabolism: regulation of gene expression, enzyme activities, and impact of genetic variation. Pharmacol Ther 138(1):103–141. https://doi.org/10.1016/j.pharmthera.2012.12.007